Direct Measurement of Room-Temperature Nondiffusive Thermal Transport Over Micron Distances in a Silicon Membrane

Jeremy A. Johnson, A. A. Maznev, John Cuffe, Jeffrey K. Eliason, Austin J. Minnich, Timothy Kehoe, Clivia M. Sotomayor Torres, Gang Chen, and Keith A. Nelson

Phys. Rev. Lett. **110**, 025901 — Published 8 January 2013

DOI: 10.1103/PhysRevLett.110.025901

Direct Measurement of Room Temperature Non-diffusive Thermal Transport Over Micron Distances in a Silicon Membrane

Jeremy A. Johnson[1]*†, A. A. Maznev[1]*, John Cuffe[2,3], Jeffrey K. Eliason[1], Austin J. Minnich[4]‡, Timothy Kehoe[2], Clivia M. Sotomayor Torres[2,5,6], Gang Chen[4], Keith A. Nelson[1].

[1]Department of Chemistry, Massachusetts Institute of Technology, Cambridge, Massachusetts 02139, USA.

[2]Catalan Institute of Nanotechnology, Campus de Bellaterra, Edifici CM7, ES 08192, Barcelona, Spain.

[3]Department of Physics, Tyndall National Institute, University College Cork, Ireland.

[4]Department of Mechanical Engineering, Massachusetts Institute of Technology, Cambridge, Massachusetts 02139, USA.

[5]Catalan Institute for Research and Advanced Studies ICREA, 08010 Barcelona, Spain.

[6]Department of Physics, Universitat Autonoma de Barcelona, 08193 Bellaterra (Barcelona), Spain.

The "textbook" phonon mean free path (MFP) of heat carrying phonons in silicon at room temperature is ~40 nm. However, a large contribution to the thermal conductivity comes from low-frequency phonons with much longer MFPs. We present a simple experiment demonstrating that room temperature thermal transport in Si significantly deviates from the diffusion model already at micron distances. Absorption of crossed laser pulses in a freestanding silicon membrane sets up a sinusoidal temperature profile that is monitored via diffraction of a probe laser beam. By changing the period of the thermal grating we vary the heat transport distance within the range ~1-10 μm. At small distances, we observe a reduction in the effective thermal conductivity indicating a transition from the diffusive to the ballistic transport regime for the low-frequency part of the phonon spectrum.

The study of thermal transport at microscopic distances [1-8] is largely stimulated by practical needs such as thermal management of microelectronic devices [2], but also poses a number of fundamental physics problems. In dielectrics and semiconductors heat is carried predominantly by phonons, and the relationship between the phonon mean free path (MFP) and a characteristic length scale determines whether the thermal transport is diffusive or ballistic. At cryogenic temperatures phonon MFPs are relatively long and ballistic phonon propagation over macroscopic distances has been studied extensively [9]. At room temperature, on the other hand, the majority of phonons have MFPs in the nanometer range. The often cited "textbook value" of the phonon MFP in Si at 273K based on a simple kinetic theory [10] is 43 nm, with even shorter MFPs listed for most other materials. According to this simplistic view one would not expect deviations from the classical thermal diffusion model at distances significantly exceeding 40 nm.

However, a growing body of experimental and theoretical studies has been indicating a large role of low-frequency phonons with MFPs much longer than tens of nanometers. Revising the "effective" room temperature phonon MFP in Si upwards to 260-300 nm has been suggested for the analysis of thermal transport in thin films [11] and superlattices [12]. Recent measurements in Si have indicated non-diffusive transport on the tens of microns distance scale at temperatures 20-100 K [7]. Still, it has been widely held that at room temperature heat transport in Si on the ~1 μm scale is consistent with diffusion theory [1].

On the theoretical side, first principles calculations of lattice thermal conductivity and phonon MFPs have emerged in recent years [8,13-16]. Although quantitative discrepancies between different models still persist, they invariably point to a large contribution of low-frequency phonons to heat transport. For example, simulations by Henry and Chen [13] have indicated that phonons with MFP exceeding 1 μm contribute almost 40% to room temperature thermal conductivity of Si.

Measuring non-diffusive thermal transport at small distances in a configuration that can be quantitatively compared to theoretical models has been a challenge for experimentalists. Theoreticians favor the model of heat transport through a slab of material between two black body walls [8,17], which is all but impossible to realize in experiment. Just to mention one difficulty, any real interface between two materials involves thermal boundary resistance, which by itself presents a long-standing problem in nanoscale thermal transport [1,18]. For a persuasive demonstration and to enable theoretical analysis beyond the diffusion model, an experiment should preferably (i) avoid interfaces, (ii) ensure one dimensional thermal transport, and (iii) clearly define the distance of the heat transfer and provide a way to vary this distance in a controllable manner. Experiments revealing non-diffusive transport on sub-micron length scales [3-5] were done with more complicated configurations involving heat transport from an irradiated film into a substrate, with the effective heat transfer distance in the substrate only indirectly inferred.

A method satisfying the above requirements has in fact been well known under the name laser-induced transient thermal gratings [19,20]. In this method, two short laser pulses are crossed in a sample resulting in an interference pattern with period L defined by the angle between the beams. Absorption of laser light leads to a spatially periodic temperature profile, and the decay of this temperature grating by thermal transport is monitored via diffraction of a probe laser beam. The heat transport from grating peaks to nulls does not involve heat transfer across any interfaces and the distance scale is controlled by the period of the optical interference pattern. An additional

advantage of the method is a spatially sinusoidal temperature profile facilitating theoretical treatment.

In this report, we present transient thermal grating measurements of in-plane heat transport in freestanding silicon membranes. By varying the grating period we are able to directly measure the effect of the heat transfer distance on thermal transport [21].

The freestanding silicon membranes were fabricated by backside etching of a silicon on insulator (SOI) wafer. In this process, the underlying Si substrate and buried oxide layer are removed through a combination of dry and wet etching techniques to leave a top layer of suspended silicon as shown in Fig. 1(a) (also see [22]). Measurements were conducted on two 400 nm thick membranes (membranes 1 and 2) with 400×400 μm^2 freestanding area fabricated on the same SOI wafer.

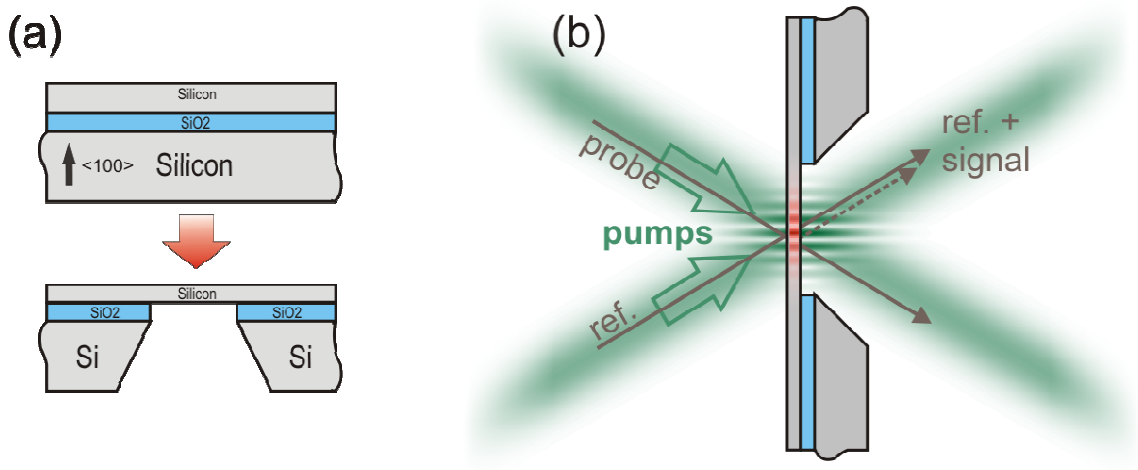

FIG. 1 (color online). Schematics of the sample and the experiment. (a) Freestanding Si membranes are fabricated from SOI wafers by backside etching. (b) Pump pulses are crossed in the silicon membrane, generating the transient thermal grating monitored via diffraction of the probe beam. Diffracted probe light is combined with a reference beam and directed to a fast detector.

Excitation laser pulses (wavelength λ_e = 515 nm, pulse duration 60 ps) were crossed in the Si membrane with external angle θ_e as depicted in Fig. 1(b). Interference between the two beams created a spatially periodic intensity and absorption pattern with interference fringe period $L=\lambda_e/2\sin(\theta_e/2)$. Above-bandgap photon absorption in the silicon membrane led to excitation of hot carriers, which promptly transferred energy to the lattice and relaxed to the bottom of the conduction band [23]. Energy was deposited with a sinusoidal intensity profile resulting in a transient thermal "grating" with period L, i.e. with carrier population and induced temperature rise modulated as $(1 + \cos qx)$ where $q = 2\pi/L$ is the grating "wavevector" magnitude; excited carriers and heat subsequently diffused from grating peaks to nulls. The membrane thickness was selected to be smaller than the ~1 μm absorption depth at the excitation wavelength to ensure one-dimensional in-plane heat transport, with the temperature gradient and heat flux only in the transient grating direction, parallel to the membrane surfaces. The measurements were performed in ambient air. The effect of the thermal conductivity of air on the thermal grating

decay in the membrane was negligible as shown by modeling heat transport in a membrane in ambient medium [22].

Increased temperature and excited carriers induced changes in the complex transmittance, giving rise to time-dependent diffraction of a continuous wave probe beam (wavelength λ_p = 532 nm). We used optical heterodyne detection whereby the diffracted signal was superposed with the local oscillator, or reference beam. Heterodyne detection not only increases the signal level but also yields a signal linear with respect to the material response that simplifies the interpretation and analysis of the data [22]. A simple set-up using a diffraction grating to produce both excitation and probe-reference beam pairs ensures the precise overlap of the probe and reference beams as well as the stability of the heterodyne phase [22,24]. The signal and reference beams were directed to a fast detector, whose output was recorded on an oscilloscope.

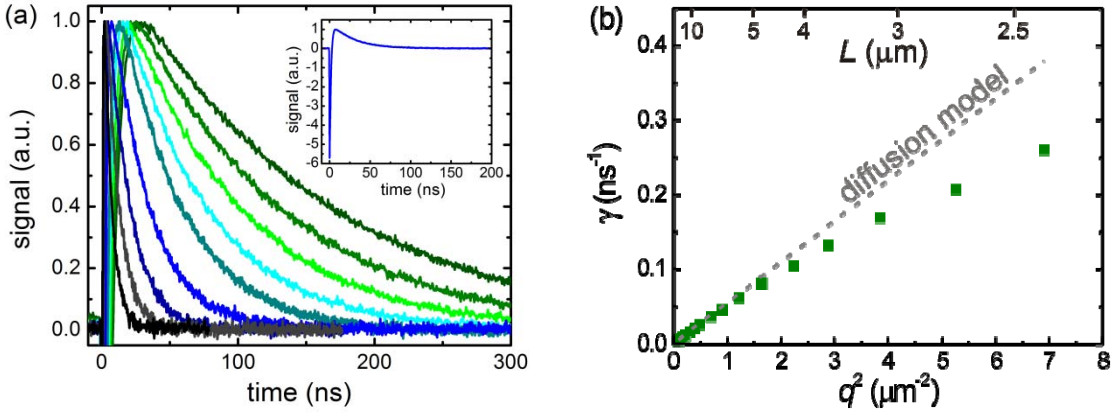

FIG. 2 (color online). Experimental data from membrane 1. (a) Thermal decay traces for transient grating periods ranging from 3.2 to 18 μm. The decay time increases with the grating period. The inset shows the complete trace for the 7.5 μm period. (b) Thermal grating decay rate versus the grating wavevector squared showing the departure from diffusive behavior. The dashed line representing the diffusion model was obtained by fitting the low-wavevector data in the range L = 15-25 μm.

Data were collected at ~15 transient grating periods ranging from 2.4 to 25 μm in the two silicon membranes. Figure 2(a) shows traces collected from membrane 1 with transient grating periods from 3.2 to 18 μm. A complete waveform shown in the inset reveals a sharp negative peak due to electronic excitation. Fortunately, the ambipolar carrier diffusion coefficient in Si is about an order of magnitude greater than the thermal diffusivity [25], therefore electronic and thermal relaxations are well separated in the time domain: after the carrier population grating is washed out due to carrier diffusion, we are left with a purely thermal grating which decays more slowly. For example, the electronic decay time seen in the inset in Fig. 2 (a) is 1.7 ns while the thermal decay time is 26 ns, as determined by a bi-exponential fit [22]. From the traces in Fig. 2(a), we can see that the thermal decay becomes slower as the grating period increases; it takes longer for heat to move from grating peaks to nulls. According to the thermal diffusion equation, the temperature perturbation decays exponentially [19], $T(x,t) \propto \cos qx \exp(-\gamma t)$, with the decay rate γ given by

$$\gamma = \alpha q^2 = kq^2/C, \qquad (1)$$

where α is the thermal diffusivity, equal to the ratio of the thermal conductivity k to the heat capacity per unit volume C.

We found that the thermal decay remains exponential within the whole range of grating periods [22]. However, the decay rate deviates from the expected q^2 dependence as can be seen in Fig. 2(b). This departure from diffusive behavior is even more apparent in Fig. 3(a) where we have plotted the effective thermal conductivity, obtained from the measured decay rate using Eq. (1), scaled by the bulk Si value, as a function of the grating period for the two membranes. At large grating periods, the thermal conductivity approaches a constant level, which is still significantly smaller than the bulk conductivity. It is well known that in-plane thermal conductivity of thin membranes is reduced due to scattering of phonons at the boundaries [11,17]. However, as long as the diffusion model is valid, the thermal grating decay rate should vary as q^2, and the measured thermal conductivity value should remain independent of the grating period. We observed a significant further reduction in the measured thermal conductivity as the grating period was reduced below about 10 μm, clearly indicating a departure from diffusive thermal transport.

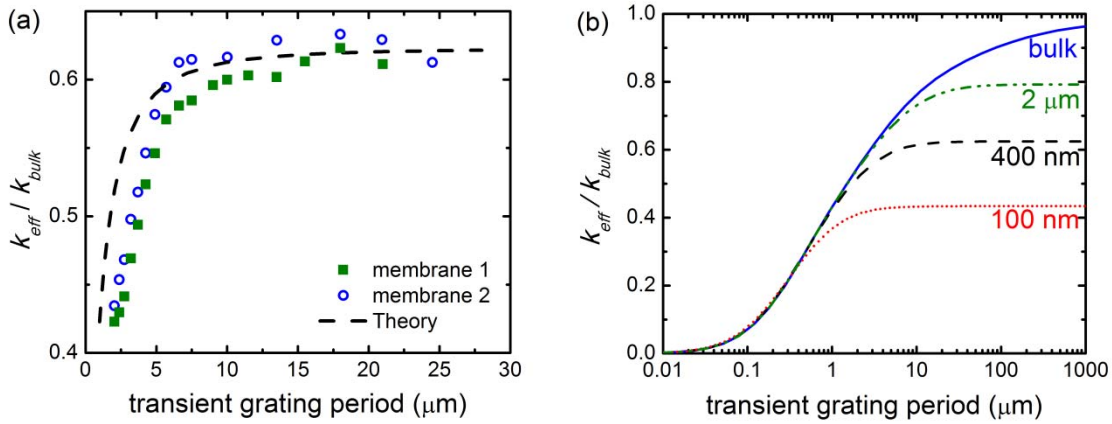

FIG. 3 (color online). (a) The normalized effective thermal conductivity versus transient grating period compared with theory. (b) The calculated effective thermal conductivity as a function of the grating period and the membrane thickness.

The decrease in the effective thermal conductivity is explained by the transition from diffusive to ballistic transport regime for the low-frequency part of the phonon spectrum. There is no contradiction with the intuitive expectation that ballistic transport should be faster than diffusive: indeed, the grating decay is always faster at shorter periods as seen directly in Fig. 2(a). However, the *increase in decay rate with wavevector* is slower than quadratic at short length scales since the traversal time of heat carried by ballistic phonons decreases linearly with distance, not quadratically as in the diffusive limit.

In the relaxation time approximation which works well for Si above ~100K [14], thermal conductivity is given by the integral over the phonon spectrum,

$$k = \frac{1}{3}\int_0^{\omega_{\max}} C_\omega v \Lambda d\omega \ , \qquad (2)$$

where C_ω is the differential frequency-dependent specific heat per unit volume, v is the phonon group velocity, Λ is the frequency-dependent MFP, and the summation over all phonon branches

is implied. According to the Fourier law of heat conduction, the contribution of phonons at a given frequency to the heat flux is given by $Q_\omega = C_\omega v \Lambda \Delta T/3l$, where l is the distance between the heat source and the heat sink and ΔT is the temperature difference. In this model the heat flux is supposed to increase indefinitely with increasing MFP, which cannot be true; obviously, it cannot exceed the purely ballistic black body radiation limit [12], $Q_{\omega\, bb} = C_\omega \Delta T/4$. Thus the contribution of ballistic phonons with $\Lambda >> l$ to thermal transport will be suppressed *at least* by a factor of $\frac{3}{4}(l/\Lambda)$ compared to the predictions of the diffusion model. In the simplest approach, the contribution of all phonons with $\Lambda > l$ is simply disregarded, while for all phonons with $\Lambda < l$ the diffusion model is assumed to hold [5,7]. In this case the "effective" thermal conductivity is found by simply cutting off the low frequency part of the integral in Eq. (2).

The simplicity of the transient grating geometry allowed us to develop a more rigorous theory of the thermal grating relaxation in a bulk material based on the Boltzmann transport equation for phonons with MFP on the order of or larger than $l = L/2$ in combination with the diffusion equation for the "thermal reservoir" of high frequency phonons with $\Lambda << l$ [26]. We found that the grating decay remains exponential with the decay rate obtained by replacing the thermal conductivity in Eq. (1) by the effective conductivity,

$$k_{eff} = \frac{1}{3}\int_0^{\omega_{\max}} A C_\omega v \Lambda d\omega$$
$$A(q\Lambda) = \frac{3}{q^2\Lambda^2}\left(1 - \frac{\arctan(q\Lambda)}{q\Lambda}\right), \qquad (3)$$

where the "correction factor" A becomes unity in the diffusive limit $q\Lambda << 1$ and falls off as $(q\Lambda)^{-2}$ in the ballistic limit $q\Lambda >> 1$. Unlike the simple "cut-off" model, Eq. (3) describes a smooth transition between diffusive and ballistic limits. The contribution of ballistic phonons to thermal transport is suppressed even more than according to the estimate based on the black body radiation limit because in the transient grating experiment the heat transport does not occur between black bodies. To the contrary, our heat "sources" and "sinks", i.e. maxima and minima of the thermal grating, become almost transparent for ballistic phonons in the limit $q\Lambda >> 1$, which accounts for an additional factor of $\sim(q\Lambda)^{-1}$ in the ballistic phonon contribution to the heat flux.

In order to calculate the effective thermal conductivity according to Eq. (3), one needs to know the phonon density of states, group velocities and relaxation times for all phonon branches. For Si at room temperature, these quantities have been computed from first principles [8,13-16]. We used the results of Ref. [13] presented in the form of thermal conductivity accumulation vs. MFP, which is particularly convenient for our purposes [22]. The calculated effective thermal conductivity for thermal grating relaxation in bulk Si is shown by the solid curve in Fig. 3(b). The effective conductivity approaches the bulk value at large grating periods and decreases at small periods. The calculation is valid under the assumption [26] that diffuse phonons with $\Lambda << L/2$ account for most of the specific heat, which holds well at $L > 1$ μm.

In a thin membrane, the effective thermal conductivity is additionally reduced by boundary scattering. The classic formula for the effective MFP in a thin film was obtained (originally for electrons) by Fuchs [27]. The rigorous analysis of the thermal grating relaxation in the presence of boundary scattering is outside the scope of this report. We estimate the combined effect of the finite heat transfer distance in the transient grating measurement and the boundary scattering in

the membrane by using the reduced MFP from the Fuchs-Sondheimer theory [28] instead of the bulk MFP in our Eq.(3) [22]. While admittedly lacking mathematical rigor, this approach yields correct results in the limiting cases when boundary scattering either dominates or is negligible. In Fig. 3(b), alongside the curve for bulk Si, we show the calculated results for three membrane thicknesses. In the large L limit the effective thermal conductivity approaches a constant value determined by the membrane surface scattering. For thinner membranes, the onset of the non-diffusive effect is shifted towards shorter grating periods. As can be seen in Fig. 3(a), the calculations for d=400 nm agree reasonably with the experiment given the uncertainties in the phonon MFP values obtained by different authors [13,14].

The fact that the deviations from the Fourier law in phonon mediated-thermal conductivity occur at much larger distances than previously thought should change the way we think of micro-scale thermal transport. One immediate implication is that accurate measurements of bulk thermal conductivity may be impossible on micron-sized samples. We have seen that the commonly cited textbook values of an "average" phonon MFP are of little relevance in analyzing the onset of size effects in thermal conductivity. Perhaps a more useful parameter would be the "median thermal conductivity MFP" Λ_m, such that phonons with $\Lambda > \Lambda_m$ contribute 50% to the bulk thermal conductivity. For Si at room temperature, calculations show this median MFP Λ_m to be ~0.5-1 μm [13,14,16]. The behavior of Λ_m will be quite different from that of the "average" MFP. For example, impurity scattering makes all MFPs shorter; however, it affects primarily high-frequency phonons. Therefore Λ_m may be in fact made larger by impurity scattering leading to larger size effects in semiconductor alloys compared to pure materials [5]. For the same reason, we may expect larger size effects in thermal transport in natural diamond than in isotopically pure diamond contrary to what has been traditionally believed [17].

This work was supported as part of the S3TEC Energy Frontier Research Center funded by the U.S. Department of Energy, Office of Basic Energy Sciences under Award DE-SC0001299/DE-FG02-09ER46577 (experimental setup and data analysis). This work was also partially supported by projects: NANOPOWER, contract 256959; TAILPHOX, contract 233883; NANOFUNCTION, contract 257375; ACPHIN, contract FIS2009-150; AGAUR, 2009-SGR-150. The samples were fabricated using facilities from the "Integrated nano and microfabrication Clean Room" ICTS funded by MICINN.

*Correspondence to: jeremy.johnson@psi.ch, maznev@mit.edu

†Current address: Paul Scherrer Institut, Villigen, Switzerland

‡Current address: California Institute of Technology, Pasadena, California

[1] D.G. Cahill, W.K. Ford, K.E. Goodson, G.D. Mahan, H.J. Maris, A. Majumdar, R. Merlin, and S.R. Phillpot. *J. Appl. Phys.* **93,** 793 (2003).

[2] E. Pop. *Nano Res.* **3**, 147 (2010).

[3] M. Siemens, Q. Li, R. Yang, K.A. Nelson, E. Anderson, M. Murnane, and H. Kapteyn. *Nature Materials* **9**, 26 (2010).

[4] M. Highland, B.C. Gundrum, Y.K. Koh, R.S. Averback, D.G. Cahill, V.C. Elarde, J.J. Coleman, D.A.Walko, E.C. Landahl. *Phys. Rev. B* **76**, 075337 (2007).

[5] Y. K. Koh, and D. G. Cahill. *Phys. Rev. B* **76**, 075207 (2007).

[6] P. G. Sverdrup, S. Sinha, M. Asheghi, S. Uma, and K. E. Goodson. *Appl. Phys. Lett.* **78**, 3331 (2001).

[7] A. J. Minnich, J.A. Johnson, A.J. Schmidt, K. Esfarjani, M.S. Dresselhaus, K.A. Nelson, G. Chen. *Phys. Rev. Lett.* **107**, 095901 (2011).

[8] D. P. Sellan, J. E. Turney, A. J. H. McGaughey, and C. H. Amon. *J. Appl. Phys.* **108**, 113524 (2010).

[9] J.P. Wolfe. *Imaging Phonons* (Cambridge University Press, Cambridge 1998).

[10] J.S. Blakemore. *Solid State Physics* (Cambridge University Press, Cambridge 1985).

[11] Y. S. Ju, K. E. Goodson. *Appl. Phys. Lett.* **74**, 3005 (1999).

[12] G. Chen. *Phys. Rev. B* **57**, 14958 (1998).

[13] A. Henry and G. Chen. *J. Comp. Theor. Nanosci.* **5**, 1 (2008).

[14] A. Ward and D. A. Broido. *Phys. Rev. B* **81**, 085205 (2010).

[15] D. A. Broido, M. Malorny, G. Birner, N. Mingo, and D. A. Stewart. *Appl. Phys. Lett.* **91**, 231922 (2007).

[16] K. Esfarjani, G. Chen, and H. T. Stokes. *Phys. Rev. B* **84**, 085204 (2011).

[17] A. Majumdar. *ASME J. Heat Transfer* **115**, 7 (1993).

[18] E.T. Swartz, R.O. Pohl. *Rev. Mod. Phys.* **61**, 605 (1989).

[19] H.J. Eichler, P. Günter, and D.W. Pohl. *Laser-Induced Dynamic Gratings* (Springer, Berlin, Heidelberg 1986).

[20] J.A. Rogers, A.A. Maznev, M.J. Banet, and K.A. Nelson. *Annu. Rev. Mater. Sci.* **30**, 117 (2000).

[21] The fact that deviations from the thermal diffusion model have not been hitherto found in transient grating measurements can be ascribed to the influence of the entrenched textbook estimates for MFP of thermal phonons. In fact, measurements similar to the ones described here (albeit without optical heterodyning) have been reported [29,30]. However, these studies used longer grating periods, which prevented detection of non-diffusive transport within the accuracy of the measurements.

[22] Further information on methods and analysis is available in the Supplementary Materials.

[23] J. R. Goldman and J. A. Prybyla. *Phys. Rev. Lett.* **72**, 1364 (1994).

[24] A. A. Maznev, J. A. Rogers, and K. A. Nelson. *Optics Letters*, **23**, 1319, 1998.

[25] C-M. Li, T. Sjodin, and H-L. Dai. *Phys. Rev. B* **56**, 15252 (1997).

[26] A. A. Maznev, J. A. Johnson, and K. A. Nelson, *Phys. Rev. B* **84**, 195206 (2011).

[27] K. Fuchs. *Proc. Cambridge Philos. Soc.* **34**, 100 (1938).

[28] E. H. Sondheimer. *Adv. Phys.* **1**, 1 (1952).

[29] M. Schmotz, P. Bookjans, E. Scheer, and P. Leiderer. *Rev. Sci. Instrum.* **81**, 114903 (2010).

[30] H.J. Eichler, F. Massmann, E. Biselli, M. Glotz, L. Konetzke, and X. Yang. *Phys. Rev. B* **36**, 3247 (1987).